# A Solution NMR Approach to the Measurement of Amphiphile Immersion Depth and Orientation in Membrane Model Systems

M. Sameer Al-Abdul-Wahid,[†] Chris Neale,[‡,§] Régis Pomès,[‡,§] and R. Scott Prosser*,[†]

*Department of Chemistry, University of Toronto Mississauga, 3359 Mississauga Road North, Mississauga, Ontario, Canada, L5L 1C6, Molecular Structure and Function, The Hospital for Sick Children, 555 University Avenue, Toronto, Ontario, Canada, M5G 1X8, and Department of Biochemistry, University of Toronto, 1 King's College Circle, Toronto, Ontario, Canada, M5S 1A8*

Received November 14, 2008; E-mail: scott.prosser@utoronto.ca

**Abstract:** Oxygen and Ni(II) are ideal paramagnetic species for NMR studies of immersion depth since they establish prominent concentration gradients across the membrane−water interface of either bilayers or micelles. Corresponding gradients of paramagnetic shifts and relaxation rates are observed by NMR for membrane embedded amphiphiles. Specifically, upon dissolution of oxygen at a partial pressure of 20 bar or more, $^{13}C$ NMR spectra of membrane embedded amphiphiles reveal chemical shift perturbations which depend sensitively on average immersion depth in the membrane. Similarly, depth-dependent enhancements of spin−lattice relaxation rates can be detected by $^1H$ NMR. Generally, such paramagnetic effects depend both on steric or accessibility factors and on the local concentration of the paramagnet. The steric terms can be factored out by combining paramagnetic rates arising from $O_2$ and Ni, in the form of a ratio, $R_{1P}(O_2)/R_{1P}(Ni)$. The natural logarithm of this ratio is shown to depend linearly on immersion depth in a micelle. The analysis is verified using molecular dynamics simulations of dodecylphosphocholine in a detergent micelle, while thorough consideration of the paramagnetic rate data also allows for the determination of the orientation of imipramine in the micelle. Thus, a complete picture of topology arises from this approach which is readily applicable to studies of drugs and amphiphiles in fast-tumbling bicelles, small unilamellar vesicles, and micelles.

## Introduction

The drug discovery process involves a myriad of measurements of the dissociation constant, $k_D$, of the molecule of interest with the active site of the target, in addition to details associated with drug Absorption, Distribution, Metabolism, and Excretion (referred to as the ADME profile). Lipophilicity of the potential drug, which may be expressed as log $P$ (*i.e.*, the logarithm of the ratio of the drug concentration in octanol to that in water) strongly influences $k_D$ and these pharmacodynamic parameters.[1,2] While there may be an optimal lipophilicity for receptor binding, other criteria include the drug's solubility, its ability to cross the gut wall membrane, and its rate of hepatic clearance, all of which relate to log $P$.[1,3] Lipophilicity is also clearly important in situations where the pharmaceutical target is a membrane protein, such as an ion channel or a G protein-coupled receptor (GPCR). It is estimated that 30% of all pharmaceuticals are designed to interact with GPCRs,[4] which are extracellular membrane receptors responsible for signal transduction across the plasma membrane. Moreover, the majority of nonpeptidic ligands for GPCRs target the cell membrane and interact with the hydrophobic transmembrane helices, making lipophilicity key to recognition of the target. Future trends in drug development for GPCR targets may well tend toward larger compounds with even greater log $P$ values at least in the case of non-aminergic GPCRs.[3] Thus, lipophilicity and membrane partitioning properties are key to both retention of the drug and the rate at which it encounters the membrane receptor. To better understand and predict a potential drug's ADME profile, details beyond the simple equilibrium information between octanol and water may be helpful, particularly in the case of amphiphiles intended for membrane receptors. In this paper we explore a solution NMR approach which can provide an accurate measure of amphiphile positioning in micelles or membrane model systems, in addition to information on orientation and water−membrane equilibria.

The determination of positioning and orientation of an amphiphilic drug in a lipid bilayer or detergent micelle requires that the majority of $^1H$ resonances can be simultaneously resolved such that a depth-dependent measurement can be performed for each resonance. $^1H$ NMR spectra of microgram quantities of small molecules can be obtained in a matter of minutes on current high field instruments (*i.e.*, $^1H$ Larmor frequencies of 500 MHz or more), particularly in cases where cryogenic probes are used.[5] Moreover, a background signal can be avoided by using perdeuterated detergents or lipids. Given sufficient spectral resolution, the position of a drug in a

† Department of Chemistry, University of Toronto Mississauga.
‡ The Hospital for Sick Children.
§ Department of Biochemistry, University of Toronto.

(1) Lipinski, C. A.; Lombardo, F.; Dominy, B. W.; Feeney, P. J. *Adv. Drug Delivery Rev.* **1997**, *23*, 3–25.
(2) Lewis, D. F. V.; Jacobs, M. N.; Dickins, M. *Drug Discovery Today* **2004**, *9*, 530–537.
(3) Beaumont, K.; Schmid, E.; Smith, D. A. *Bioorg. Med. Chem. Lett.* **2005**, *15*, 3658–3664.
(4) Blakeney, J. S.; Reid, R. C.; Le, G. T.; Fairlie, D. P. *Chem. Rev.* **2007**, *107*, 2960–3041.

membrane can be ascertained by a variety of approaches. For example, substantial chemical shift perturbations are observed upon transfer of the ligand of interest from water to the micelle or membrane model.[6] Typically, upfield shifts signify burial of corresponding ^{1}H nuclei in the hydrophobic interior, although chemical shift perturbations are well-known to depend on a host of factors such as local conformation, dynamics, and/or specific interactions with the membrane headgroup.[6] Similarly, [1]H Nuclear Overhauser Effects (NOEs), which involve through-space magnetization exchange between ^{1}H nuclear spins belonging to lipids or detergents and the embedded drug, may be used to establish the relative positioning of amphiphiles in (proto-nated) membranes or micelles,[7−9] although such interproton contacts are confounded by spin diffusion and extensive lipid and amphiphile dynamics.[9,10] In some cases, water NOEs[11,12] may be helpful in establishing positioning of amphiphiles in membrane models.[6,13] However, water NOEs to nuclei in the membrane interior are typically weak and do not correlate well with immersion depth.

**Paramagnetic Probes for the Determination of Immersion Depth in Membrane Models.** Depth-specific effects from paramagnetic additives are a useful alternative to chemical shift perturbations or intermolecular NOEs in studies of drug positioning in membrane models. For example, lipid or fatty acid amphiphiles bearing nitroxide spin labels at a specific position on the aliphatic chain or headgroup give rise to pronounced line broadening or spin−lattice relaxation enhancement on ^{1}H nuclei in the vicinity of the spin label.[8,14] In principle such effects may extend to average separations, $r$, of 20 Å (between nuclear spin and paramagnet), and a gradation of such effects is expected to follow a $1/r^6$ dependence. Although somewhat tedious, a series of such paramagnetic probes, each separately confined to a small range of immersion depths, may be used to establish positioning in the membrane of various resolvable drug nuclei. A further concern is the possibility that the nitroxide group on the paramagnetic additive preferentially interacts with certain sites on the amphiphile under study, thus biasing the results.

Oxygen has been shown to be an extremely sensitive paramagnetic additive in studies of positioning in membrane models.[15−17] At partial pressures of 20 bar, oxygen establishes pronounced concentration gradients and corresponding paramagnetic effects, across the water−micelle or water−membrane interface, extending to the hydrophobic center of the membrane.[18] In contrast to depth studies which employ a series of

nitroxide paramagnetic probes, the broad concentration gradient associated with $O_2$ allows for the assessment of depth from a single sample. Moreover, useful pressures (20−50 bar) are easy to achieve with the aid of commercially available glass or sapphire NMR tubes, and it is equally straightforward to remove the paramagnet by gently degassing the sample. Calorimetric and spectroscopic studies have shown that pressure can affect physical properties of membranes, although such effects are generally observed at pressures of hundreds of atmospheres or more.[17,19,20] Potential effects of pressure arising from the use of oxygen at partial pressures 20−50 bar can be reliably accounted for by running control measurements under equivalent $N_2$ partial pressures. Prior NMR experiments in membrane model systems, using $N_2$ rather than $O_2$, have shown that pressure effects are negligible.[15] Effects of sample oxidation are in some cases a concern, although such effects can be prevented by buffering the sample pH near 7 and by addition of 20 mM dithiothreitol.

Paramagnetic effects of oxygen may be observed in the form of depth-specific shifts, line broadening, or $T_1$-relaxation enhancement. Chemical shift perturbations, which have been utilized in ^{13}C and ^{19}F NMR applications,[15,21−23] and to a lesser extent in ^{15}N and ^{1}H NMR, arise solely from a contact mechanism due to the fact that the oxygen molecule is diffusing and tumbling rapidly, relative to the molecule of interest, thereby avoiding any pseudocontact (dipolar) shift effects.[23,24] Under such circumstances, the contact shift is found to depend primarily on the local oxygen concentration and on the extent of accessible surface area. Ideally, such shift measurements would be obtained from the difference of paramagnetic shifts observed in a membrane model to those in water [i.e., $\Delta\delta_{O_2}(membrane) - \Delta\delta_{O_2}(H_2O)$]. In this way, paramagnetic shifts may be corrected for effects that depend simply on the local bond type (i.e., sp, sp$^2$, or sp$^3$ in the case of ^{13}C shifts) rather than on the local environment. Recently,[23] ^{13}C NMR paramagnetic shift measurements arising from dissolved oxygen were used to compare solvent exposure in a folded and compact unfolded state of a soluble protein. Large shifts were found to highlight solvent-exposed areas, and a lack of such shifts indicated clustering of residues. In the case of membranes, the situation is different in the sense that we rely on a pronounced $O_2$ concentration gradient to understand immersion depth of all resolvable nuclei in the amphiphile under study.

A second way of accurately assessing immersion depth via $O_2$ paramagnetic effects is through changes in the spin−lattice relaxation rate upon oxygenation [i.e., $R_{1p} = R_1(O_2) - R_1(ambient)$]. Unlike paramagnetic shift effects, pronounced paramagnetic relaxation rate enhancements have proven useful in topology and membrane immersion studies involving ^{19}F and ^{1}H nuclei. A detailed analysis of such paramagnetic rates, expressed in terms of a steric factor, $f$, associated with accessibility of the paramagnet to the nuclear spin, the local

(5) Voehler, M. W.; Collier, G.; Young, J. K.; Stone, M. P.; Germann, M. W. *J. Magn. Reson.* **2006**, *183*, 102–109.

(6) Evanics, F.; Prosser, R. S. *Anal. Chim. Acta* **2005**, *534*, 21–29.

(7) Losonczi, J. A.; Olejniczak, E. T.; Betz, S. F.; Harlan, J. E.; Mack, J.; Fesik, S. W. *Biochemistry* **2000**, *39*, 11024–11033.

(8) Hilty, C.; Wider, G.; Fernandez, C.; Wuthrich, K. *ChemBioChem* **2004**, *5*, 467–473.

(9) Feller, S. E.; Brown, C. A.; Nizza, D. T.; Gawrisch, K. *Biophys. J.* **2002**, *82*, 1396–1404.

(10) Huster, D.; Gawrisch, K. *J. Am. Chem. Soc.* **1999**, *121*, 1992–1993.

(11) Dalvit, C.; Hommel, U. *J. Magn. Reson., Ser. B* **1995**, *109*, 334–338.

(12) Dalvit, C.; Hommel, U. *J. Biomol. NMR* **1995**, *5*, 306–310.

(13) Gawrisch, K.; Gaede, H. C.; Mihailescu, M.; White, S. H. *Eur. Biophys. J. Biophys. Lett.* **2007**, *36*, 281–291.

(14) Dzikovski, B. G.; Livshits, V. A.; Marsh, D. *Biophys. J.* **2003**, *85*, 1005–1012.

(15) Prosser, R. S.; Luchette, P. A.; Westerman, P. W. *Proc. Natl. Acad. Sci. U.S.A.* **2000**, *97*, 9967–9971.

(16) Evanics, F.; Hwang, P. M.; Cheng, Y.; Kay, L. E.; Prosser, R. S. *J. Am. Chem. Soc.* **2006**, *128*, 8256–8264.

(17) Prosser, R. S.; Luchette, P. A.; Westerman, P. W.; Rozek, A.; Hancock, R. E. W. *Biophys. J.* **2001**, *80*, 1406–1416.

(18) Marsh, D. *Proc. Natl. Acad. Sci. U.S.A.* **2001**, *98*, 7777–7782.

(19) Mateo, C. R.; Tauc, P.; Brochon, J. C. *Biophys. J.* **1993**, *65*, 2248–2260.

(20) Molina-Garcia, A. D. In *Biotechnology & Genetic Engineering Reviews, Vol 19*; Intercept Ltd Scientific, Technical & Medical Publishers: Andover, 2002; Vol. 19, pp 3 ff.

(21) Evanics, F.; Kitevski, J. L.; Bezsonova, I.; Forman-Kay, J. D.; Prosser, R. S. *Biochim. Biophys. Acta* **2007**, *1770*, 221–230.

(22) Bezsonova, I.; Korzhnev, D. M.; Prosser, R. S.; Forman-Kay, J. D.; Kay, L. E. *Biochemistry* **2006**, *45*, 4711–4719.

(23) Bezsonova, I.; Evanics, F.; Marsh, J. A.; Forman-Kay, J. D.; Prosser, R. S. *J. Am. Chem. Soc.* **2007**, *129*, 1826–1835.

(24) Prosser, R. S.; Luchette, P. A. *J. Magn. Reson.* **2004**, *171*, 225–232.

concentration of oxygen, $[O_2]$, and a distance of closest approach, $b$, may be given as[25]

$$R_{1p} = \frac{32\pi}{405}\gamma_I^2\gamma_S^2\hbar^2 S(S+1)\frac{N_A f}{1000}\frac{[O_2]}{bD}\{j_2(\omega_S - \omega_I) + 3j_1(\omega_I) + 6j_2(\omega_I + \omega_S)\} \quad (1)$$

where $\gamma_I$ and $\gamma_S$ are the gyromagnetic ratios of the nuclear spin, $I$, and electron spin, $S$; $\omega_I$ and $\omega_S$ are Larmor frequencies of nuclear and electron spins; $N_A$ is Avogadro's constant; and $D$ is the relative translational diffusion constant. Note that the above expression is derived assuming free isotropic diffusion with a uniform diffusion coefficient $D$. In the case of a membrane–water interface one would expect $D$ to change, leaving the validity of the expression in question for this application. For the moment, we assume that $D$ does not change significantly in the vicinity of a single nuclear spin of interest, and we note that we will ultimately be considering a ratio of paramagnetic rates in the final analysis. Also note that the spectral density term, $\{j_2(\omega_S - \omega_I) + 3j_1(\omega_I) + 6j_2(\omega_I + \omega_S)\}$, which describes the fluctuations of the $I$–$S$ dipole coupling, is dominated by the picosecond time scale electron spin relaxation which is constant. Thus, $R_{1p}$ is primarily sensitive to the local oxygen concentration and to accessibility or topology, rather than a combination of dynamics and topology.[26–31]

**Distinguishing Steric Effects from Depth-Specific Effects with Paramagnetic Additives.** The measurement of depth-dependent effects via $O_2$-induced ^{1}H and ^{19}F NMR paramagnetic rates or ^{13}C and ^{19}F NMR paramagnetic shifts has been successfully applied to studies of amphiphiles and membrane proteins in membrane model systems.[15,16,32,33] However, a precise measurement of immersion depth via the local depth-specific concentration, $[O_2(z)]$, can only be made once the local steric or accessibility factors can be taken into account. One approach to this problem is to complement paramagnetic rates from $O_2$ with additional paramagnetic rate measurements from a small freely diffusing water-soluble paramagnet, such as Ni(II), or its chelated form, Ni(II) acetylacetonate (NiAcac). NiAcac preferentially partitions into the aqueous phase and exhibits a concentration profile, $[Ni(z)]$, which is essentially the opposite of $[O_2(z)]$. This approach was first taken in Electron Spin Resonance (ESR) applications where it was recognized that local paramagnetic effects of either oxygen or Ni(II) could together be used to resolve immersion depth of spin-labeled lipids or membrane proteins.[34–36] Ni(II) is a convenient paramagnetic probe and is complementary to $O_2$ in part because it possesses

very short electronic spin relaxation times and is thus suited to a similar description for NMR paramagnetic rates, as given above. To a first approximation one would expect paramagnetic rates arising from either $O_2$ or Ni(II) to reflect similar steric factors. Hence, the ratio of paramagnetic rates due to $O_2$ and Ni(II), $R_{1p}(O_2)/R_{1p}(Ni)$, should be proportional to the ratio of the local concentrations, $[O_2(z)]/[Ni(z)]$, which in turn depends sensitively on immersion depth as discussed below.

Formally, we define the immersion depth, $z$, as the distance from the micelle center. As this is a somewhat nebulous definition, we would in practice always relate immersion depth measurements to a known standard, usually atoms of the lipid or detergent headgroup. The concentration of some paramagnetic additive, $i$, at a depth, $z$, may be expressed in terms of the standard state chemical potentials, $\mu_{i,w}^0$ and $\mu_{i,m}^0(z)$ associated with the aqueous and membrane-like phases respectively, giving[35]

$$C_{i,m}(z) = C_{i,w}\exp(\mu_{i,w}^0/RT)\exp(-\mu_{i,m}^0(z)/RT) \quad (2)$$

where $C_{i,w}$ is the uniform concentration of species $i$ in bulk water. We next define the natural logarithm of the ratio of paramagnetic rates, $\Phi$, as follows

$$\Phi(z) \equiv \ln\left[\frac{R_{1p}(O_2)}{R_{1p}(Ni)}\right] \quad (3)$$

Since the electronic spin–lattice relaxation times for both $O_2$ and Ni(II) are extremely short and do not vary considerably throughout the sample,[25] the spectral density terms appearing in eq 1 are effectively decoupled from other, slower dynamics, in which case the only variables in the above expression for $R_{1p}$ become the steric terms ($f$ and $b$) and the local paramagnet concentration (*i.e.*, $[O_2(z)]$ or $[Ni(z)]$). Assuming the variation in the relative diffusion rate, $D$, is much less significant than that of the paramagnet concentration, the ratio of paramagnetic rates will be proportional to the ratio of paramagnet concentrations [i.e., $C_{O_2,m}(z)/C_{Ni,m}(z)$]. Thus, referring to eq 2 we can express the depth dependent parameter, $\Phi(z)$, in terms of the difference of the chemical potentials of $O_2$ and Ni in the micelle, and a constant, *const*, giving[35]

$$\Phi(z) = -\left(\mu_{O_2}^0(z) - \mu_{Ni}^0(z)\right)/RT + const \quad (4)$$

Note that the bulk NiAcac and $O_2$ concentrations should independently be chosen to offer a maximum range of effects across the membrane– or micelle–water interface, without compromising spectral resolution. For our purposes, ideal NiAcac concentrations are ∼1 mg/mL and ideal $O_2$ concentrations are obtained upon equilibrating at a partial pressure of 30 bar. Clearly, the relative choice of bulk concentrations dictates the magnitude of $C_{O_2,m}(z)/C_{Ni,m}(z)$. However, our interest is in obtaining a sensitive measure of depth [*i.e.*, $\Phi(z)$], in which case different choices of relative bulk concentrations of the two paramagnetic additives simply give rise to different values for *const* in eq 3, for concentrations used in these experiments.

Herein, we test the validity of the approach of combining ^{1}H paramagnetic rate measurements from dissolved $O_2$ and NiAcac in the form of the above-mentioned depth-dependent profile, $\Phi(z)$, to determine the immersion depth of membrane amphiphiles. We then compare this approach to the depth fidelity of other biophysical approaches. We consider imipramine, a well-known tricyclic anticholinergic antidepressant which interacts strongly with micelles (log $D$ = 2.3)[37] as a test compound, and we correlate experimentally measured immer-

(25) Teng, C. L.; Hinderliter, B.; Bryant, R. G. *J. Phys. Chem. A* **2006**, *110*, 580–588.
(26) Teng, C. L.; Bryant, R. G. *J. Am. Chem. Soc.* **2000**, *122*, 2667–2668.
(27) Hernandez, G.; Teng, C. L.; Bryant, R. G.; LeMaster, D. M. *J. Am. Chem. Soc.* **2002**, *124*, 4463–4472.
(28) Ulmer, T. S.; Campbell, I. D.; Boyd, J. *J. Magn. Reson.* **2002**, *157*, 181–189.
(29) Teng, C. L.; Bryant, R. G. *Biophys. J.* **2004**, *86*, 1713–1725.
(30) Ellena, J. F.; Moulthrop, J.; Wu, J.; Rauch, M.; Jaysinghne, S.; Castle, J. D.; Cafiso, D. S. *Biophys. J.* **2004**, *87*, 3221–3233.
(31) Sakakura, M.; Noba, S.; Luchette, P. A.; Shimada, I.; Prosser, R. S. *J. Am. Chem. Soc.* **2005**, *127*, 5826–5832.
(32) Luchette, P. A.; Prosser, R. S.; Sanders, C. R. *J. Am. Chem. Soc.* **2002**, *124*, 1778–1781.
(33) Al-Abdul-Wahid, M. S.; Yu, C. H.; Batruch, I.; Evanics, F.; Pomes, R.; Prosser, R. S. *Biochemistry* **2006**, *45*, 10719–10728.
(34) Altenbach, C.; Marti, T.; Khorana, H. G.; Hubbell, W. L. *Science* **1990**, *248*, 1088–1092.
(35) Altenbach, C.; Greenhalgh, D. A.; Khorana, H. G.; Hubbell, W. L. *Proc. Natl. Acad. Sci. U.S.A.* **1994**, *91*, 1667–1671.
(36) Hubbell, W. L.; Gross, A.; Langen, R.; Lietzow, M. A. *Curr. Opin. Struct. Biol.* **1998**, *8*, 649–656.
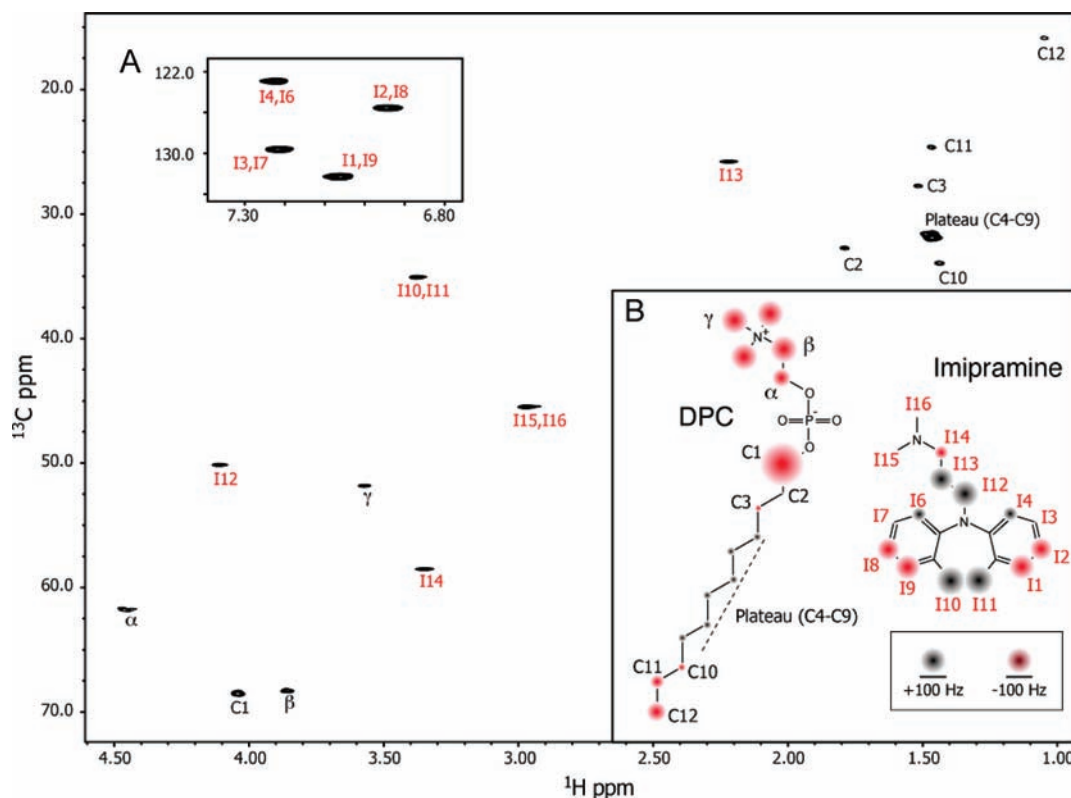
**Figure 1.** (A) Assigned [$^{13}$C,$^1$H] HSQC spectrum of imipramine in DPC micelles at 30 °C. (B) Inset: The $^{13}$C chemical shift changes upon transfer from the free to micelle-bound state ($\Delta\delta_{transfer}^{C13}$, as described in eq 5) are presented as spheres overlaid over the structures of DPC and imipramine. Transfer shifts for I3/I7 and I15/I16 are less than 10 Hz.

sion depths to molecular dynamics derived immersion depths of the resident dodecylphosphocholine (DPC) micelle nuclei.

## Results and Discussion

The fast tumbling of detergent micelles (as compared to larger aggregates such as bicelles or small unilamellar vesicles) allows for complete resolution of imipramine resonances (by $^{13}$C and $^1$H NMR) and substantial resolution of DPC resonances, where the only overlap occurs in the "plateau" region of C4–C9 which are represented as a single peak in the [$^{13}$C,$^1$H] HSQC, shown in Figure 1. Figure 1B depicts the structural formulas of DPC and imipramine in which the $^{13}$C chemical shift perturbations resulting from transfer from the free state to the micellar state are graphically overlaid. Here, the chemical shift changes upon transfer from the free state to the micelle (designated by the subscript *trnsfr*, below) are defined as

$$\Delta_{trnsfr}^{C13} \equiv \delta_{micelle}^{C13} - \delta_{free}^{C13} \qquad (5)$$

Clearly, the transfer shifts prove sensitive to the change of environment or topology, though not particularly sensitive to immersion depth since there does not appear to be a prominent gradient of $\Delta\delta_{transfer}^{C13}$ across the membrane–water interface, nor are the shifts even of the same sign. We therefore consider the use of paramagnetic additives (NiAcac and O$_2$) whose partitioning properties in membranes and micelles essentially amplify subtle differences in environment, through either contact shifts or paramagnetic relaxation rate enhancements.

**Paramagnetic Chemical Shift Perturbations.** $^{13}$C and $^1$H chemical shift perturbations, $\Delta\delta_{O_2}^{C13}$ and $\Delta\delta_{O_2}^{H1}$ of DPC and

imipramine, resulting from the dissolution of O$_2$ equilibrated to a partial pressure of 30 bar, are shown in Figure 2. In contrast to the relatively scattered chemical shift profile associated with the transfer from water to micelle, the prominent gradient of chemical shift perturbations is a consequence of the pronounced O$_2$ concentration gradient and underlies the potential of O$_2$ to distinguish immersion depth.[33,38] Note that $\Delta\delta_{O_2}^{C13}$ increases monotonically from 14.4 Hz (0.096 ppm) at the DPC headgroup to 133.5 Hz (0.89 ppm) for the terminal methyl in DPC, while $\Delta\delta_{O_2}^{H1}$ similarly extends between 7.2 Hz (0.012 ppm) and 102 Hz (0.17 ppm). The chemical shift perturbations associated with the micellar detergent help to establish a reference for positioning imipramine in the micelle. Based on the relative magnitude of paramagnetic shifts, we propose that the drug is oriented such that the tricyclic ring system is closest to the micelle center and the "tail" of imipramine extends outward to the micelle–water interface.

**Paramagnetic Rate Enhancements.** Figure 3 displays paramagnetic $^1$H spin–lattice relaxation rates, $R_{1P}(O_2)$ and $R_{1P}(Ni)$, associated with molecular oxygen (Figure 3A) and NiAcac (Figure 3B), which are obtained simply from the difference of the spin–lattice relaxation rates in the presence of paramagnet from those under ambient conditions. Note that paramagnet concentrations have been chosen to maximize depth-dependent effects without undue line broadening. In contrast to oxygen, NiAcac preferentially partitions into the bulk aqueous phase, and its effects drastically decrease toward the micelle interior (Figure 4). Corresponding rates reflect this concentration gradient; $R_{1P}(Ni)$ ranges from 2.15 Hz at the α position of DPC to

(37) Frisk-Holmberg, M.; van der Kleijn, E. *Eur. J. Pharmacol.* **1972**, *18*, 139–147.

(38) Prosser, R. S.; Evanics, F.; Kitevski, J. L.; Patel, S. *Biochim. Biophys. Acta* **2007**, *1768*, 3044–3051.
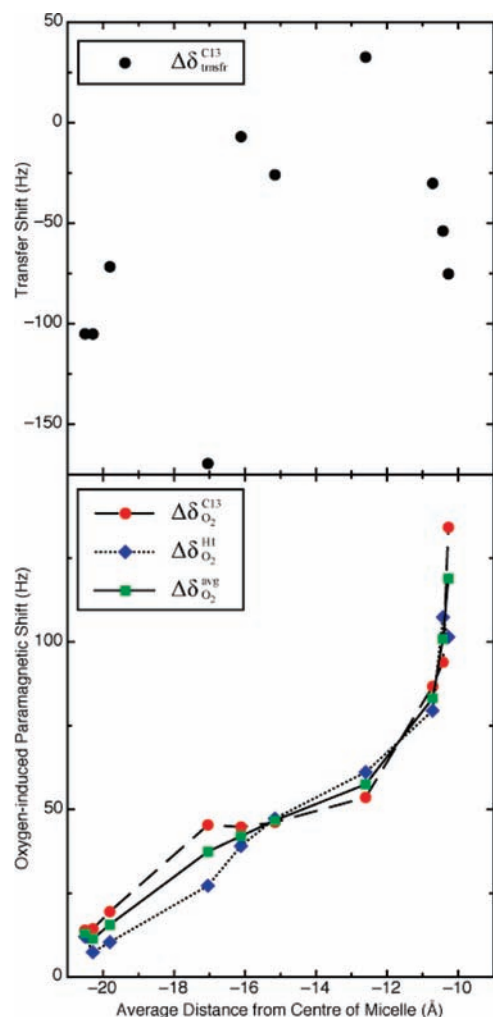
**Figure 2.** $^{13}C$ and $^{1}H$ NMR paramagnetic shifts, $\Delta\delta_{O_2}^{C13}$ and $\Delta\delta_{O_2}^{H1}$, resulting from the dissolution of $O_2$ after equilibrating at a partial pressure of 30 bar, graphed as a function of MD-derived average distance from the micelle center, $z$, for DPC. An average paramagnetic shift is defined by $\Delta\delta_{O_2}^{avg} = [\{(\Delta\delta_{O_2}^{C13})^2 + (\Delta\delta_{O_2}^{H1})^2\}/2]^{1/2}$. Shown for comparison in the upper panel the chemical shift changes, $\Delta\delta_{transfer}^{C13}$, associated simply with transfer from water to the micelle.

0.35 Hz for the terminal methyl on the acyl chain. The high error in the paramagnetic rate measurements associated with the $\alpha$, $\beta$, and C1 protons of DPC is due to a particularly low

signal-to-noise ratio for these peaks, attributed to extremely high levels of deuteration at these sites. As noted in the Materials and Methods section, the relaxation measurements are performed on the residual 1% of protons in 99% perdeuterated DPC and certain sites have higher levels of deuteration than others (data not shown).

In all studies of topology in membranes in which paramagnetic additives are used, we must contend with both steric effects which relate to the local accessibility of the paramagnet to the nuclear spin of interest, in addition to the depth (topology) dependent effects which are the focus of this paper. As discussed in the introduction, the ratio of paramagnetic rates associated with $O_2$ to those associated with NiAcac should cancel out steric effects, leaving a measure of immersion depth for each resolvable spin. The extent to which such a ratio serves as a measure of depth can be tested by comparing the experimental quotient, $\Phi(z) \equiv \ln[(R_{1P}(O_2))/(R_{1P}(Ni))]$, for all DPC resonances. The exact immersion depths of the DPC nuclei can in turn be independently verified by molecular dynamics (MD) simulations of DPC in a micellar state. Figure 5 plots the experimental depth parameter, $\Phi(z)$, as a function of MD-determined immersion depth for DPC. Note that there is a strong linear correspondence between $\Phi(z)$ and the MD-determined depths ($R^2 = 0.988$). These $\Phi(z)$ values may then be used as internal reference points with which to assess the immersion depth of resolvable $^{1}H$ nuclei within imipramine. As shown in Figure 5, the immersion depths of $^{1}H$ nuclei associated with all resolvable resonances on imipramine in the micelle were determined directly from the reference line generated by DPC, with no additional fitting parameters.

**Orientation of Imipramine in the Micelle.** Based on the above $\Phi(z)$ analysis, the heptane ring CH_2 groups (I10,I11) and the four adjacent CH groups (I1,I2,I8,I9) flanking the CH_2 groups are closest to the micelle center, while the methyl groups at the other end of imipramine (I15,I16) are in the vicinity of the detergent headgroups. To determine the average angle of imipramine with respect to the micelle normal, we consider the two major conformations of imipramine[39] and compare the interatomic distances in these conformations to the experimentally determined immersion depths. This method also serves to ensure that the experimentally determined immersion depths are consistent (and possible) with the known structure. To illustrate this method, consider that, over the two major conformations of imipramine, the average length of imipramine along its
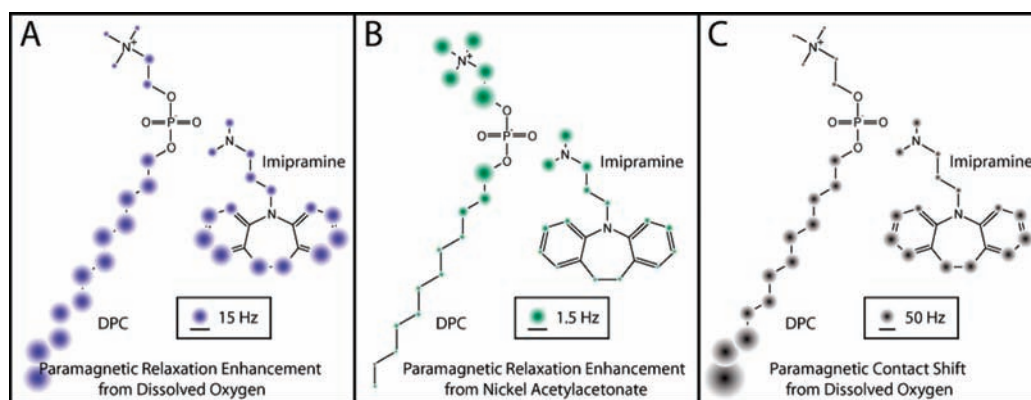


**Figure 3.** A graphical comparison of the paramagnetic relaxation rate enhancements ($R_{IP}$) on $^{1}H$ nuclei of DPC and imipramine due to $O_2$ (A) and NiAcac (B). $O_2$-induced paramagnetic shifts on $^{13}C$ nuclei under identical conditions are shown in C. A scale is provided at the bottom of the each figure. Note that spheres in B have been magnified by a factor of 10 in diameter relative to those in A due to the relatively small rate effects seen at this concentration of NiAcac.
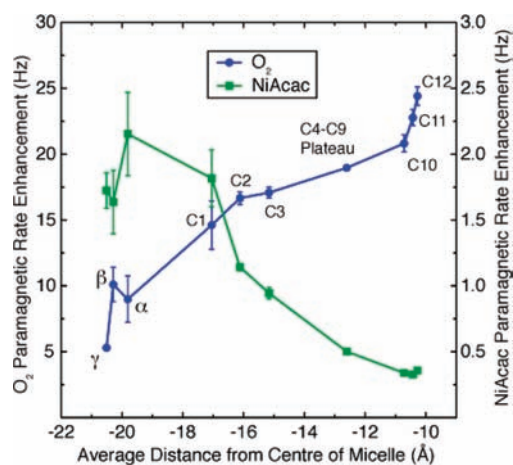
**Figure 4.** [1]H paramagnetic relaxation rate enhancements ($R_{1P}$) of DPC arising from dissolved $O_2$ (30 bar) and NiAcac (1 mg/mL). The solubility gradients of $O_2$ and NiAcac give rise to corresponding gradients in the $R_{1P}$ profiles, with $R_{1P}(O_2)$ increasing and $R_{1P}(NiAcac)$ decreasing toward the micelle center.



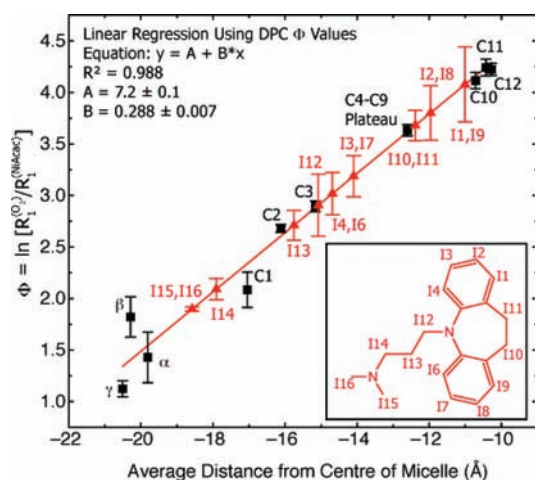**Figure 5.** Experimentally determined immersion depth parameter, $\Phi(z)$ $\equiv \ln[(R_{1P}(O_2))/(R_{1P}(Ni))]$, graphed as a function of MD-derived depth, $z$, for DPC (black squares) and imipramine (red triangles). Here, DPC serves as a reference with which to place imipramine.

symmetry axis (as defined by the distance between the average positions of the protons on I15/I16 and I1/I9) is 8.9 Å.[39] The experimentally determined range of immersion depths (Figure 5) spans only 8.15 Å, suggesting that imipramine adopts a nonzero angle with respect to the micelle normal. The tilt angle is most accurately measured by employing a least-squares fitting routine using all observable sites on imipramine to determine the tilt angle at which the known conformations would produce the observed immersion depths when placed in a micelle. In this case we obtain an average orientation of the imipramine symmetry axis, $\theta = 29° \pm 3°$, which is equivalent to a local molecular order parameter, $S$, of 0.65 and a cone angle of 41° $\pm 4°$ if the "wobble-in-a-cone" model is used to consider the motion of imipramine in the micelle. Figure 6B illustrates the orientational analysis and the subsequent model for the positioning of imipramine in the micelle.

**A Comparison to Conventional Approaches.** ESR studies have used an identical approach to determine immersion depth

(39) Post, M. L.; Kennard, O.; Horn, A. S. *Acta Crystallogr., Sect. B* **1975**, *31*, 1008–1013.
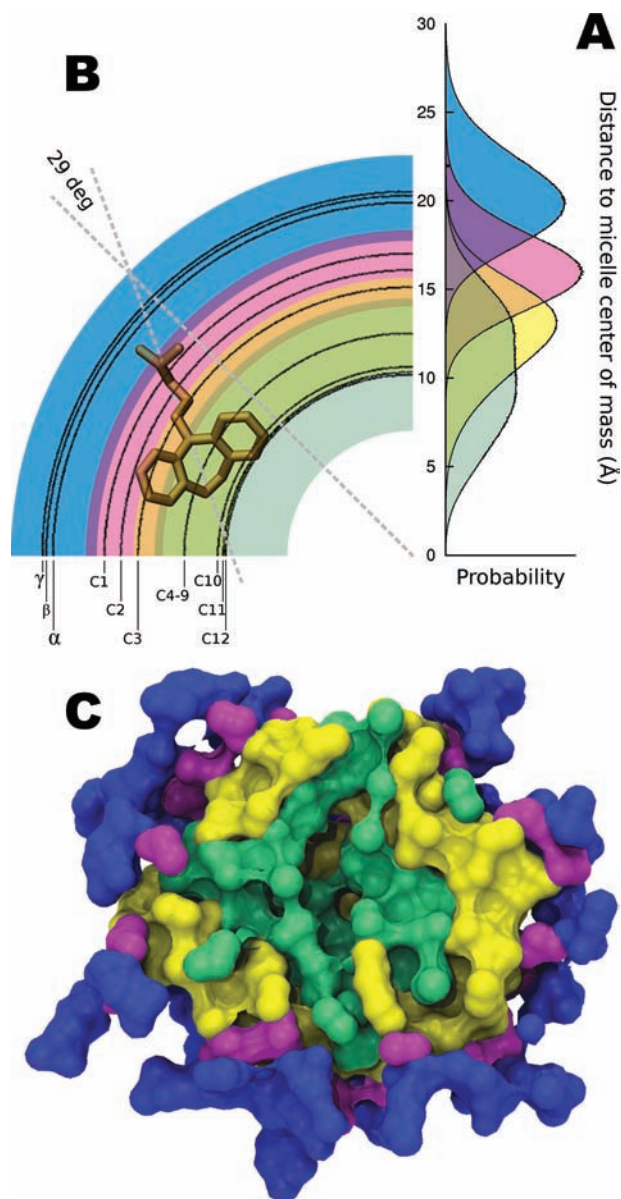


**Figure 6.** Spatial properties of a DPC micelle calculated from MD simulation. (A) Distribution of time-averaged distances to the micelle center of mass for selected DPC groups. Distances sampled by carbons in the choline headgroup, C1−C3, C4−C9, and C10−C12 are colored blue, magenta, yellow, and light green, respectively. (B) Circular projection of the most heavily sampled 66% of distances for each DPC group. Black lines indicate the average distance to the micelle center of mass sampled by each NMR-resolved carbon atom(s). Plots A and B are drawn to relative scale. The average orientation of imipramine (29° ± 3°) is overlaid on plot B. (C) A cross section through a randomly selected snapshot from the MD simulation of DPC; the coloring scheme is the same as that in A and B with the addition of the headgroup nitrogen and phosphorus atoms (shown in blue).

profiles and, thus, topologies of membrane peptides and membrane proteins.[35] In such studies, a protein is usually tagged at a site of interest via a nitroxide spin label which is in turn attached to a labile cysteine residue. The resulting ESR line widths and saturation-recovery times turn out to be extraordinarily sensitive to the local concentration of paramagnetic relaxation agents such as Ni(II) or $O_2$ to a much greater extent than that observed by NMR. Moreover, pronounced paramagnetic effects from $O_2$ are observed under ambient conditions. This relates to the fact that the ESR Larmor frequency nearly coincides with

the electron spin relaxation rate, such that very low concentrations of either Ni(II) or $O_2$ give rise to significant effects. A complete immersion depth profile for a membrane protein is obtained from an exhaustive series of single cysteine mutants, in which local dynamics is assessed by ESR line widths while topology can be ascertained by measuring the residue-specific effects of $O_2$ and Ni(II) on ESR saturation rates.[34,36,40–42] Such experiments can be performed on complex lipid bilayer mixtures and at very low protein (probe) concentrations, in contrast to NMR. However, the ESR measurements also have inherent limitations. Paramagnetic effects in ESR are dominated by the so-called Heisenberg spin exchange and thus depend sensitively on the collisional frequency with the paramagnet, *i.e.* the product of the relative diffusion coefficient of the paramagnet with respect to the spin-label and the paramagnet concentration, $C_{i,m}(z)$.[35] Thus, analysis is potentially complicated by two depth-dependent variables: diffusion rate and concentration. Moreover, ESR spin labels (and the obligatory cysteine mutants) are potentially sterically and functionally perturbing. These limitations are particularly problematic in studies of small molecules, where the spin label may drastically alter the positioning of the amphiphile in the membrane, while it is simply not practical to obtain detailed immersion depth information across the entire span of a small molecule.

NMR is ideally suited to the study of amphiphile positioning in membranes. Though larger concentrations of $O_2$ or Ni(II) are required to see relaxation or chemical shift effects on nearby nuclei in contrast to ESR applications with the identical additives, line broadening is also typically modest in relation to the relative changes in spin−lattice relaxation rates for membrane embedded amphiphiles. Thus, spectral resolution is adequate for the study of paramagnetic effects on many resonances at once. Second, paramagnetic effects of $O_2$ or Ni(II) are relatively easy to interpret quantitatively. Similarly, the paramagnetic shifts depend on a steric term and on the local concentration. Finally, NMR has the advantage that the reporter of the local $O_2$ or Ni concentration is simply a nuclear spin and may include $^{13}C$, $^1H$, $^{19}F$, and other nuclei.

## Conclusions

In this study, $^1H$ paramagnetic spin−lattice relaxation rates arising from dissolved NiAcac or $O_2$ proved to be sensitive to immersion depth. NiAcac and, to an even greater extent, $O_2$ are seen as amplifiers of environment in the sense that their innate concentration gradients help to establish a reliable measure of immersion depth through paramagnetic shifts or, more commonly, paramagnetic rates. Similar experiments have been performed via fluorescence quenching[43] and ESR[34,36,40–42] in which identical paramagnetic additives may be used. In the case of NMR, the probe is simply a nuclear spin (ideally $^1H$ or $^{19}F$, though similar but weaker effects are observed with low gamma nuclei). Thus, the methodology outlined above is amenable to studies of immersion depth and topology of peptides and small molecules, where conventional methods that make use of bulky probes are not applicable. It is also fortuitous that

the selected paramagnets are somewhat weak relaxation agents for NMR. Analysis is thus straightforward, and many resonances can be simultaneously considered given the relatively weak line broadening accompanying these measurements. Finally, when coupled with a molecular dynamics simulation of the detergent micelle, the ratio $\Phi(z) \equiv \ln[(R_{1P}(O_2))/(R_{1P}(Ni))]$ proved to be exquisitely sensitive to immersion depth. A closer inspection of the unique $^1H$ immersion depths revealed that orientation (or equivalently, a molecular order parameter) could also be determined for the amphiphile under study. Thus, a complete picture of topology arises from this approach which is completely applicable to studies of drugs and amphiphiles in fast tumbling bicelles,[44] small unilamellar vesicles, and micelles.

## Materials and Methods

Perdeuterated dodecylphosphocholine (DPC) and deuterium oxide were used as obtained from Cambridge Isotope Laboratories (Cambridge, OH). Imipramine hydrochloride was used as obtained from ICN Biomedicals Inc. (Aurora, OH), and nickel acetylacetonate (NiAcac) was used as obtained from Sigma Chemicals (Mississauga, ON). DPC micelles were prepared by dissolving 114 mg of DPC in 780 $\mu$L of 50 mM phosphate buffer (pH 7) in $D_2O$. 1.1 mg of imipramine hydrochloride was then added to the micelles, resulting in a drug/detergent ratio of 1:100. The sample was thoroughly stirred and vortexed for several minutes after which a transparent, homogeneous mixture was obtained.

All NMR experiments were performed on a 600 MHz Varian Inova spectrometer and a triple resonance liquids probe, at a temperature of 303 K. The standard [$^{13}C$,$^1H$] HSQC experiment was converted to a $T_1$-HSQC by the addition of a proton $\pi$ pulse and inversion recovery period, $\tau$, prior to the start of the HSQC sequence. Eight $\tau$ values, ranging from 0.001 to 2 s, were used for $T_1$-measurements in the absence of a paramagnetic additive, while a series of ten $\tau$ values ranging from 0.002 to 0.5 s or eight values ranging from 0.01 to 1.5 s were used in the presence of $O_2$ and NiAcac, respectively. Typical HSQC spectra were acquired with 16 scans and 200 increments in the indirect dimension, spanning 12000 Hz. HSQC spectra of the aromatic region of imipramine were acquired in separate experiments, with 16 scans and 50 increments in the indirect dimension, spanning 6000 Hz. $^{13}C$ and $^1H$ oxygen-induced chemical shift perturbations ($\Delta\delta_{O_2}^{C13}$ and $\Delta\delta_{O_2}^{H1}$) were obtained by subtracting the appropriate chemical shift of a sample pressurized to an oxygen partial pressure of 30 bar from those of a sample at atmospheric pressure. Paramagnetic relaxation enhancements from oxygen and NiAcac were obtained by subtracting the spin−lattice relaxation rate in the absence of any paramagnetic additive from the rate obtained under a partial oxygen pressure of 30 bar or with the addition of 1 mg/mL NiAcac. Spectra were processed with the NMRPIPE processing suite.[45] Typically, FID signals consisting of 512 complex points in the direct dimension were zero-filled to 2048 points along with squared-cosine apodization before Fourier transformation. In the indirect dimension, FID signals consisting of 200 complex points were linearly predicted to 400 points and zero-filled to 1600 points along with squared-cosine apodization before Fourier transformation.

**MD Simulations of a DPC Micelle.** The initial structure of a DPC micelle ($N = 54$) was taken from Tieleman et al.[46] Simulations were conducted with version 3.3.1 of the GROMACS simulation package,[47] using the Berger parameters for DPC[48] and solvating

(40) Hubbell, W. L.; Altenbach, C. *Curr. Opin. Struct. Biol.* **1994**, *4*, 566–573.

(41) Cordero-Morales, J. F.; Cuello, L. G.; Zhao, Y. X.; Jogini, V.; Cortes, D. M.; Roux, B.; Perozo, E. *Nat. Struct. Mol. Biol.* **2006**, *13*, 311–318.

(42) Cuello, L. G.; Cortes, D. M.; Perozo, E. *Science* **2004**, *306*, 491–495.

(43) Bronshtein, I.; Afri, M.; Weitman, H.; Frimer, A. A.; Smith, K. M.; Ehrenberg, B. *Biophys. J.* **2004**, *87*, 1155–1164.

(44) Vold, R. R.; Prosser, R. S.; Deese, A. J. *J. Biomol. NMR* **1997**, *9*, 329–335.

(45) Delaglio, F.; Grzesiek, S.; Vuister, G. W.; Zhu, G.; Pfeifer, J.; Bax, A. *J. Biomol. NMR* **1995**, *6*, 277–293.

(46) Tieleman, D. P.; van der Spoel, D.; Berendsen, H. J. C. *J. Phys. Chem. B* **2000**, *104*, 6380–6388.

(47) Lindahl, E.; Hess, B.; van der Spoel, D. *J. Mol. Model.* **2001**, *7*, 306–317.

(48) Berger, O.; Edholm, O.; Jahnig, F. *Biophys. J.* **1997**, *72*, 2002–2013.

with 8483 TIP4P water molecules.[49] Periodic boundary conditions were enforced via a rhombic dodecahedron unit cell with an initial minimum distance of 1.5 nm between the solute and the boundary. Lennard−Jones interactions were evaluated using a group-based twin-range cutoff[50] calculated every step for separation distances less than 0.9 nm and every ten steps for distances between 0.9 and 1.4 nm, when the nonbonded list was updated. Coulomb interactions were calculated using the smooth particle-mesh Ewald method[51,52] with a real-space cutoff of 0.9 nm and a Fourier grid spacing of 0.12 nm. Simulation in the NpT ensemble was achieved by isotropic coupling to a Berendsen barostat[53] at 1 bar with a coupling constant of 4 ps and separate coupling of the solute and the solvent to Berendsen thermostats[53] at 303 K with coupling constants of 0.1 ps. Bonds involving hydrogen were constrained with SETTLE[54]

and LINCS[55] for solvent and solute, respectively. The integration time step was 2 fs. The system was simulated for 82 ns, and coordinates were saved every 1 ps. Distances between a DPC carbon type and the center of mass of the micelle were averaged over 2−82 ns, and the standard error of the mean was determined based on 20 ns segments of the trajectory.

**Supporting Information Available:** Tabulated immersion depths and Φ values for DPC and imipramine. This material is available free of charge via the Internet at http://pubs.acs.org.

JA808964E

(49) Jorgensen, W. L.; Chandrasekhar, J.; Madura, J. D.; Impey, R. W.; Klein, M. L. *J. Chem. Phys.* **1983**, *79*, 926–935.
(50) Vangunsteren, W. F.; Berendsen, H. J. C. *Angew. Chem., Int. Ed. Engl.* **1990**, *29*, 992–1023.
(51) Darden, T.; York, D.; Pedersen, L. *J. Chem. Phys.* **1993**, *98*, 10089–10092.
(52) Essmann, U.; Perera, L.; Berkowitz, M. L.; Darden, T.; Lee, H.; Pedersen, L. G. *J. Chem. Phys.* **1995**, *103*, 8577–8593.
(53) Berendsen, H. J. C.; Postma, J. P. M.; Vangunsteren, W. F.; Dinola, A.; Haak, J. R. *J. Chem. Phys.* **1984**, *81*, 3684–3690.
(54) Miyamoto, S.; Kollman, P. A. *J. Comput. Chem.* **1992**, *13*, 952–962.
(55) Hess, B.; Bekker, H.; Berendsen, H. J. C.; Fraaije, J. *J. Comput. Chem.* **1997**, *18*, 1463–1472.